Optical Materials 72 (2017) 590–595

Contents lists available at ScienceDirect

Optical Materials

journal homepage: www.elsevier.com/locate/optmat

# Novel report on γ-glycine crystal yielding high second harmonic generation efficiency

Mohd Anis [a, *], S.P. Ramteke [a], M.D. Shirsat [b], G.G. Muley [a], M.I. Baig [c]

[a] Department of Physics, Sant Gadge Baba Amravati University, Amravati, 444602, Maharashtra, India
[b] RUSA Centre for Advanced Sensor Technology, Dr. Babasaheb Ambedkar Marathwada University, Aurangabad, 431005, Maharashtra, India
[c] Prof Ram Meghe College of Engineering and Management, Amravati, 444701, Maharashtra, India

ARTICLE INFO

*Article history:*
Received 17 June 2017
Received in revised form
30 June 2017
Accepted 3 July 2017

*Keywords:*
γ-glycine crystal
Optical studies
Nonlinear optical materials
Electrical studies
X-ray diffraction

ABSTRACT

Present investigation very firstly reports the growth of γ-glycine crystal from aqueous solution containing cesium chloride. The crystallographic data of γ-glycine crystal has been experimentally determined by means of single crystal X-ray diffraction (XRD) technique. The powder XRD technique has been employed to examine the crystalline nature and structural parameters of grown crystal. The element detection has been achieved by means of energy dispersive spectroscopic technique. The color centered luminescence behavior of γ-glycine crystal has been analyzed in the range of 300–700 nm. The UV–visible study has been carried out within 200–1100 nm to determine the optical transparency and optical band gap of grown crystal. The second harmonic generation (SHG) efficiency of γ-glycine crystal has been determined by means of Kurtz-Perry test and the SHG efficiency is found to be 5.06 times higher than standard potassium dihydrogen orthophosphate crystal material. The dielectric parameters of grown crystal have been evaluated at different temperature and frequencies. The grown crystal has been subjected to differential thermal analysis to determine the melting point of γ-glycine crystal.


## 1. Introduction

In current era of science and technology design and growth of nonlinear optical (NLO) crystals has emerged as rapidly developing field owing to its practical demand in photonic industries. Organic crystals inheriting fast electro-optic effects, wide bonding network for design flexibility and high nonlinear susceptibility pronounces its credibility for fabricating second harmonic generation (SHG), optical modulation, frequency mixing, optical switching and optical parametric oscillation devices [1–4]. Looking at the growing interest of researchers in organic NLO materials the crystal of small amino acid glycine draws more attention owing to abundance of unique and interesting features. The most enticing property of glycine that cites attention is polymorphism. Hitherto, reports on crystal of α [5], β [6] and γ [7] polymorph of glycine are available. At room temperature two polymorphs of glycine are stable out of which α-glycine crystal belongs to centrosymmetric space group ($P2_1/_c$) and γ-glycine crystal belongs to noncentrosymmetric space group ($P3_1/P3_2$) [8]. The designing/tuning of laser assisted NLO devices demands material with unique set of linear and nonlinear optical properties which shrinks circumference of our research to γ-glycine crystal and exclude α-glycine owing to lack of acentric symmetry. γ-glycine orients with noncentrosymmetric space group and this guarantees the occurrence of promising NLO effects. The γ-glycine crystal is further known to be crystallized with trigonal hemihedral [9] or hexagonal [10] symmetry which makes it more interesting crystal to study. In past few decades attempts have been made to grow γ-glycine crystal that offers high conversion efficiency. The γ-glycine crystal grown using additives lithium hydroxide, lithium nitrate [11], lithium bromide [12], potassium fluoride [13], potassium nitrate [14] lithium acetate [15] and sodium sulphate [16] are reported to have sufficiently high second harmonic generation (SHG) efficiency. However, quest for obtaining more SHG efficient γ-glycine crystal is still on verge which has been trailed in current investigation. In this communication our group very firstly reports the growth of γ-glycine crystal using cesium chloride as additive. Noteworthy fact is that the γ-glycine crystal delivered the highest SHG efficiency (5 × KDP). Therefore the studies on grown γ-glycine crystal have been accomplished by employing X-ray diffraction, energy dispersive spectroscopy, UV–visible, Kurtz-Perry test, luminescence, dielectric and thermal

* Corresponding author.
*E-mail addresses:* loganees@gmail.com, loganees@yahoo.com (M. Anis).

http://dx.doi.org/10.1016/j.optmat.2017.07.007
0925-3467/

characterization techniques.

## 2. Experimental procedure

The starting materials (glycine and cesium chloride) of high purity (SDfine make) were selected with double distilled water to synthesize the γ-glycine crystal employing the conventional slow solvent evaporation technique. Initially 1 wt% of cesium chloride was dissolved in 100 ml of water and stirred for half hour. The glycine salt (1 mol) was gradually added to the prepared aqueous solution of cesium chloride and stirred well for 4 h to facilitate the formation of homogeneous mixture. This solution was later filtered through membrane filter paper (4 μm pore size) using the vacuum pump. The filtrate was transferred in clean rinsed beaker and covered with the perforated coil to avoid the dust inclusions and control the evaporation of the filtrate. The beaker was kept in a constant temperature bath at 35 °C to employ uniform and slow evaporation of solvent. The beaker was constantly observed till good quality crystals were obtained. The 17 × 10 × 06 $mm^3$ single crystal of γ-glycine (GG) grown within three weeks is shown in Fig. 1a. The purity of material was further achieved by repetitive recrystallization process.

## 3. Results and discussion

The GG crystal was subjected to single crystal X-ray diffraction analysis to record the crystallographic data at room temperature and the powder XRD (PXRD) technique to confirm the crystalline phase and confirm the cell parameters of grown crystal. The PXRD pattern (Fig. 1b) of GG crystal was recorded at the scan rate of $0.1^{\theta}$ constrained within 2θ range of $10–50^{\theta}$. The PXRD pattern was indexed and the cell parameters were evaluated using the powderX software keeping the error limit of $0.01^{\theta}$. The presence of defects/inclusions/grain boundaries results to decrease in intensity and widening of diffraction peaks. The sharp diffraction peak and less full width half maxima (FWHM) affirm the good crystalline nature of material conclusive in plane wave dynamical theory of X-ray diffraction [17,18]. Analysis of PXRD pattern plotted in Fig. 1b shows prominent and sharp diffraction peaks of characteristic (100), (110) and (111) planes of GG crystal. The evident high intensity and sharpness of identified peaks confirm that the GG crystal is free from structural grain boundaries [19,20]. In both the XRD analysis the GG crystal is found to have crystallized with hexagonal crystal structure and the cell parameters of GG crystal is tabulated in Table 1. The structural parameters of grown GG crystal are in agreement with JCPDS data (File No.06-0230) and reported work [21].

The qualitative analysis of GG crystal has been undertaken by means of energy dispersive spectroscopic (EDS) technique using the Hitachi S4700 instrument. The single crystal was powdered and the EDS spectrum of same material has been recorded in the energy range of 0–10 KeV. The peaks observed at different energies corresponding to the constituent elements present in crystal are indexed in spectrum as shown in Fig. 2a. It is notable observation that there was no trace of cesium in grown GG crystal.

The photoluminescence (PL) is the most unique nondestructive and decisive technique employed to probe the nature of electronic transition to different energy states while photo-relaxation of material later to photo-excitation. The trajectory of electron transition during photo-relaxation gives rise to characteristic color centered PL emission. Hence examination of this process becomes vital aspect to investigate the surface quality, electronic purity and influence of defects in given crystalline medium [22–25]. The PL emission spectrum of grown GG crystal has been recorded using the Hitachi FL-7000 spectrophotometer with excitation and emission slit width constrained to 2.5 nm. The material was photo-excited at the energy wavelength of 271 nm corresponding to the energy of 4.58 eV and the PL emission spectrum was recorded in the range of 300–700 nm at a scan speed of 240 nm/s with zero delay and response time was set at 0.1 s. The PL emission spectrum depicted in Fig. 2b reveals that the GG crystal contributes prominent PL emission with peak maxima centered at 343 nm (3.62 eV) resembling the violet color emission. Similar violet colored emission at 380 nm was observed in GG crystal grown from aqueous solution of lithium hydroxide [11]. In biomedical, chemical and biochemical research fields the specific PL emission profile beholds huge impetus for detection of distinct compounds [26,27]. The occurrence of defects and impurities facilitate additional states for electrons and holes which tunes the transition energies, trajectory and lifetime of electron [28]. However presence of single peak, smooth spectrum, sharp intensity and gradual decrease in intensity of PL emission confirm the absence of defects and intermediate transitions in GG crystal which pronounces its electronic purity and makes it a potential candidate for aforesaid applications.

In an optically active material the linear optical transmittance is attributed by permitted electronic transitions in band structures [29,30] which originates as a consequence of absorption of incident light of threshold energy. However, the transmittance in bulk crystal is influenced by external factors such as crystal orientation [31], defects, inclusions, impurities, vacancies, voids and grain

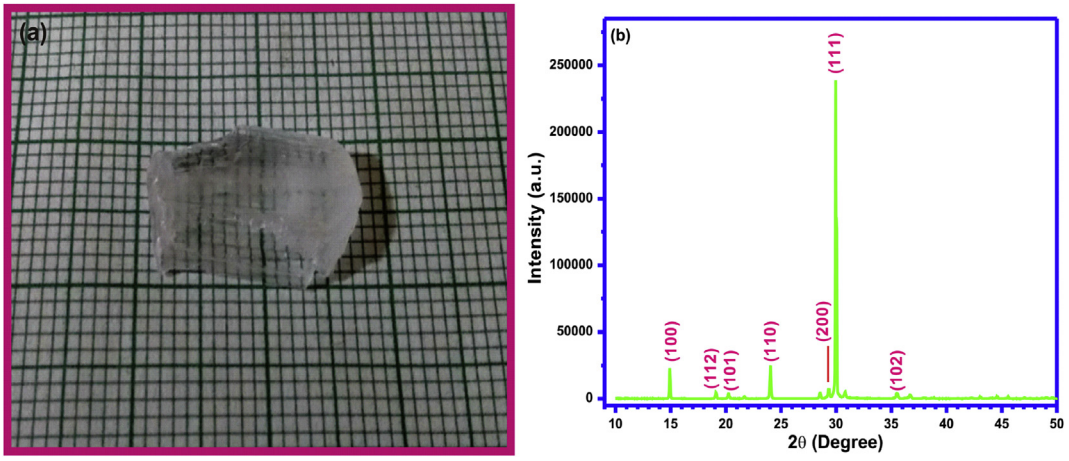


**Fig. 1.** (a) γ-glycine crystal (b) PXRD pattern of GG crystal.

**Table 1**
Structural data of γ-glycine crystal.

| Crystal parameter | Single crystal XRD | Powder XRD |
|---|---|---|
| Cell dimensions | a = b = 7.0213 Å, c = 5.4517 Å<br>α = 90°, β = 90°, γ = 120° | a = b = 7.0211 Å, c = 5.4514 Å<br>α = 90°, β = 90°, γ = 120° |
| Cell volume (Å)$^3$ | 233.738 Å$^3$ | 233.712 Å$^3$ |
| Crystal system | Hexagonal | Hexagonal |
| Space group | $P3_1$ | $P3_1$ |
| Z | 3 | 3 |

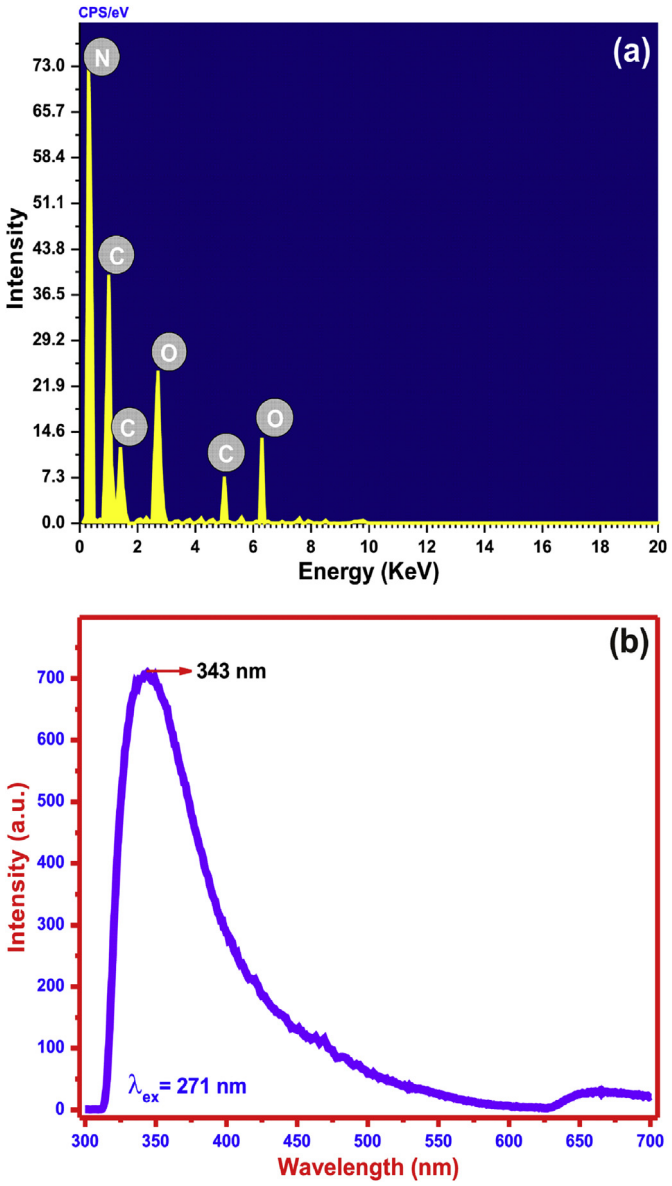


**Fig. 2.** (a) EDS and (b) PL emission spectrum of GG crystal.

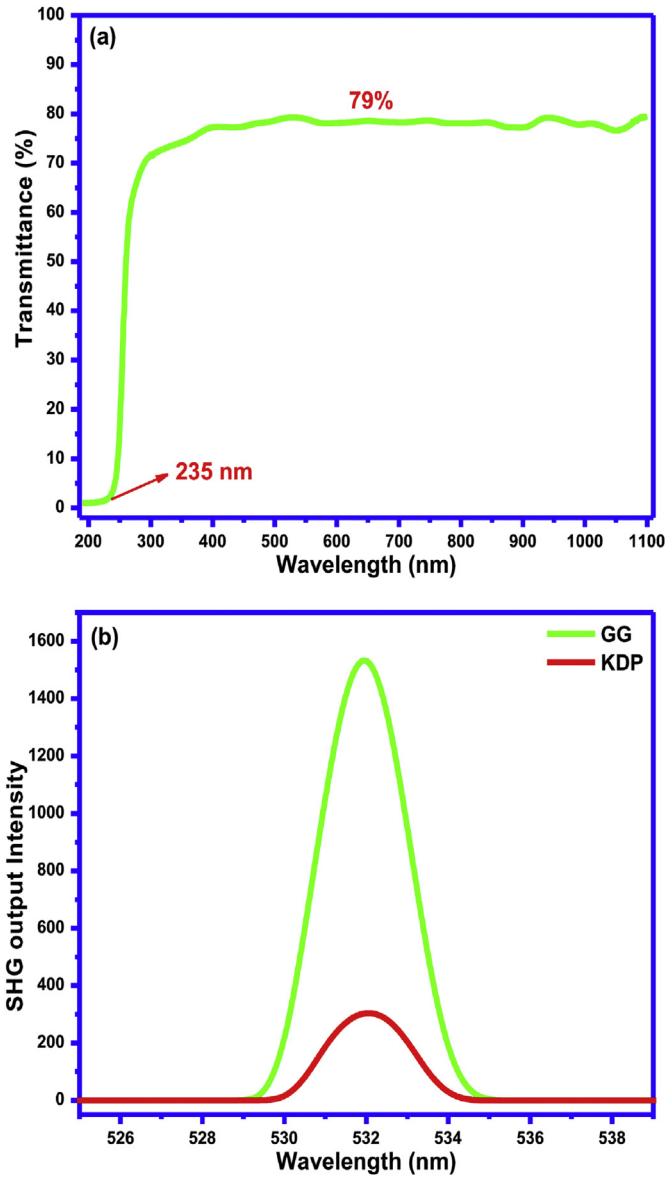


**Fig. 3.** (a) UV–visible transmittance spectrum (b) Intensity dependent SHG response.

boundaries [32,33]. These factors collectively determine the operative range and percentage of transmittance of given crystal. The materials with high transmittance are desirable for purpose of NLO applications. In order to testify that the GG crystal (2.5 mm thickness) has been scanned in the range of 200–1100 nm using the Shimadzu UV-1061 spectrophotometer and the recorded transmittance spectrum is shown in Fig. 3a. The observation of spectrum reveals that GG crystal offers transmittance of 79% and the fall in transmittance to minimum value owing to n-π transition confirms its cut-off wavelength ($\lambda_{cut\text{-}off}$) at 235 nm. In crystals grown at low temperature there is more possibility of dwelling solvent inclusions and impurities which foster structural and crystalline defects in crystallite. Notable uniform and high transmittance by GG crystal throughout the spectral range might have been contributed by inherent less absorption tendency of glycine [34] and lesser density of defect centers which minimizes the internal scattering/

absorption of light [35,36] and increases the intensity of transmittance. Also the sharp fall of transmittance in lower wavelength range determines the excellent optical homogeneity of GG crystal. The knowledge of optical band gap ($E_g = 1242/\lambda_{cut\text{-}off}$) determines the wide transmission range of given material which is found to be 5.28 eV for GG crystal. The striking linear optical parameters make the GG crystal most potential candidate for designing components utilized in transmission of harmonic signals of Nd:YAG laser, NLO and optoelectronic devices [37–39].

The standard Kurtz-Perry powder test technique [40] has been employed to determine the conversion efficiency of GG crystal. The SHG setup facilitated with Q-switched mode Nd:YAG laser (1064 nm, 6 ns, 10 Hz) has been used to determine the SHG efficiency of crystal. The alpha glycine, GG and potassium dihydrogen orthophosphate (KDP) were grounded to powder of identical size and systematically sieved in the quartz cavity. The samples were placed in optical path and the setup was initiated to irradiate the samples by Gaussian filtered beam of Nd:YAG laser. The frequency doubling phenomenon was not observed in alpha glycine owing to lack of asymmetric structure as reported [41]. On the contrary the emergence of green light was observed for GG and KDP sample which confirms the second order NLO behavior. The output intensity contributed by each sample was collected through the optical fiber and recorded using the spectrophotometer (Black-C-SR Stellar Net) interfaced to computer. The experimentally determined SHG output intensity is shown in Fig. 3b and the SHG efficiency of GG crystal is found to be 5.06 times higher than KDP crystal. The noncentrosymmetric orientation, high dipole moment and enhanced charge transfer over the acceptor-donor network are the principle factors responsible for SHG efficiency in glycine [11,42]. In addition two factors might serve significant role in favoring large SHG efficiency (i) the disordering of crystal structure in organic materials leads to generation of large electronic infrared bands below the energy gap. These infrared bands facilitate trapping of electrons and manifest more electron-phonon interaction which play active role in dwelling the photoinduced nonlinear response [43–45] and (ii) the additive cesium chloride is expected to facilitate more polarizing medium which favors more reaction sites and increases the possibility of forming more noncentrosymmetric structural symmetry which is desirable parameter for gaining SHG efficiency. The knowledge of these effects establishes the concrete ground for attaining such high SHG efficiency in grown GG crystal. The SHG efficiency of GG crystal is compared with literature in Table 2. The highest SHG efficiency of GG crystal amongst compared crystals lifts its credibility and possibility to be utilized in laser frequency doubling/conversion device applications [46].

The dielectric parameters of the materials are tunable and sensitive to applied external frequency and temperature. Therefore, the dielectric measurement studies of flat and polished GG crystal has been carried out using the HIOKI-3532 LCR instrument. The measurements have been carried out by varying the frequency (100 Hz, 100 KHz, 1 MHz) and employing the change in temperature from 35 to 80 °C. In crystal medium the contributions from electronic, ionic, dipolar and space charge polarizations give rise to the property of dielectric constant [47]. The variation in dielectric constant of GG crystal is shown in Fig. 4a. It reveals that the dielectric constant decreases with increase in frequency and increases with rise in temperature. The high magnitude of dielectric constant at 100 Hz is contributed by active polarizations at lower frequency amongst which space charge polarization becomes more dominant with increase in temperature [48]. The common effect encountered in crystal is that the polarization activity becomes less responsive at higher frequencies [49] even the space charge polarization is diminished beyond frequency of 1 KHz [50]. This justifies the large fall in magnitude of dielectric constant of GG crystal with increase in frequency from 100 Hz to 1 MHz. The lower magnitude of dielectric constant at higher frequencies implies that the GG crystal consume less power which designates it as potential candidate for applications in THz wave generation, optoelectronics, photonics, electro-optic modulators and field detectors devices

**Table 2**
Comparison of SHG efficiency of GG crystals.

| Solvent additive with water | SHG efficiency | Crystal structure | Reference |
|---|---|---|---|
| Lithium hydroxide | 1.4 (KDP) | Hexagonal | [11] |
| Lithium bromide | 3 (KDP) | Trigonal | [12] |
| Potassium fluoride | 3 (KDP) | Hexagonal | [13] |
| Potassium nitrate | 2.06 (KDP) | Hexagonal | [14] |
| Lithium acetate | 3.4 (KDP) | Hexagonal | [15] |
| Sodium chloride | 2 (KDP) | Hexagonal | [15] |
| Sodium nitrate | 1.6 (KDP) | Hexagonal | [15] |
| Sodium sulphate | 1.7 (KDP) | Hexagonal | [16] |
| Cesium chloride | 5.06 (KDP) | Hexagonal | Present study |

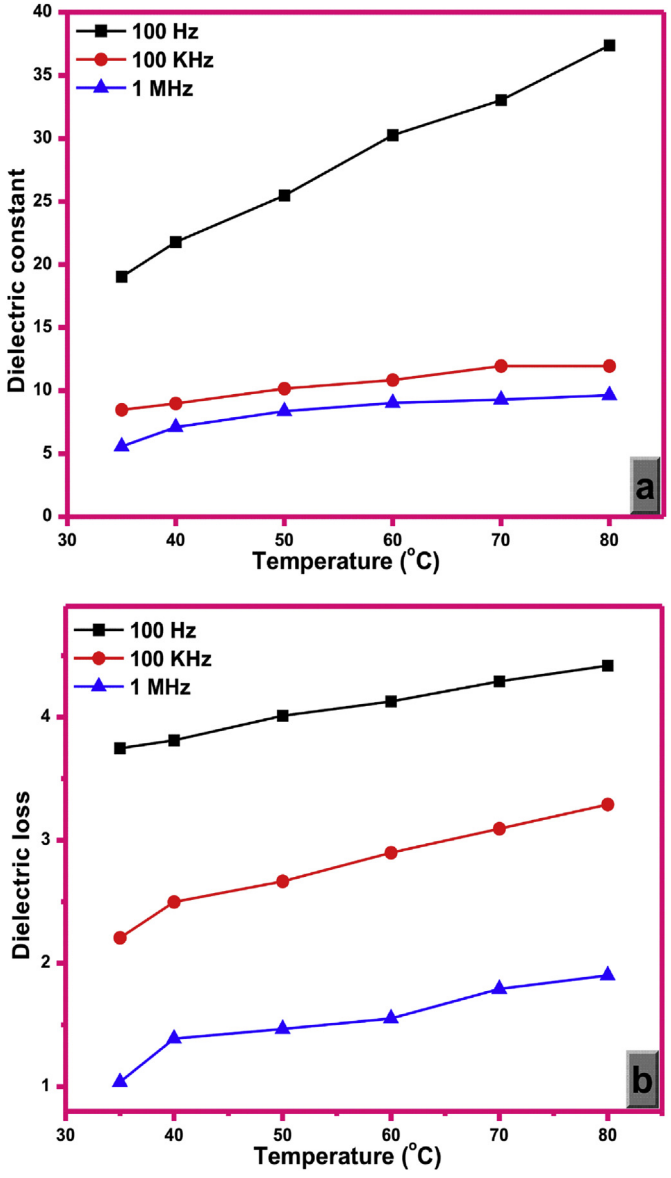


**Fig. 4.** Response of (a) dielectric constant (b) dielectric loss.

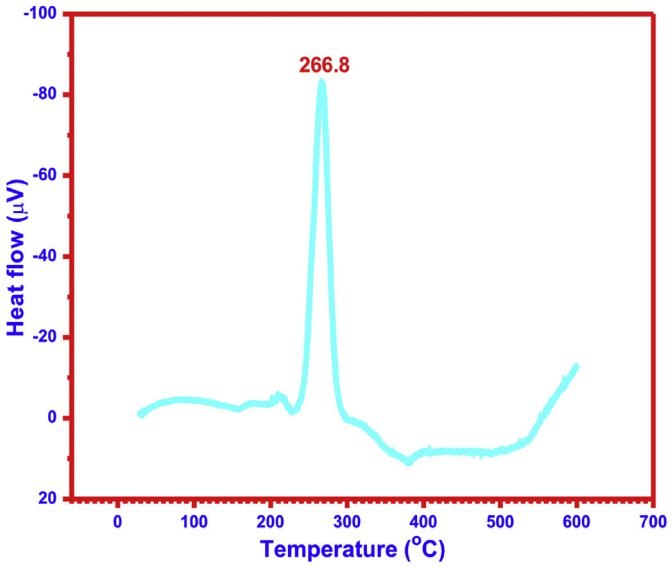


**Fig. 5.** DTA curve of GG crystal.

[51–53]. Conclusive studies of Miller revealed that the materials with less dielectric constant contribute higher SHG efficiency [54] which is true in case of grown GG crystal. The dielectric loss is the essential parameter of the material which evaluates the loss of electromagnetic signal in crystal medium. The major factors giving rise to dielectric loss are intrinsic phonon interactions and extrinsic defects (impurities, inclusion, porosity, vacancies, grain boundaries, micro-macro cracks, random crystal growth) [55,56]. The variation of dielectric loss is shown in Fig. 4b. It depicts that the dielectric loss decreases with increase in frequency. The low value of dielectric loss at higher frequency confirms excellent quality of crystal with less electrically active defects [57,58]. The promising dielectric behavior of GG crystal advocates its credibility for engineering distinct technological device.

As continuous laser exposure creates thermal conductivity in crystal medium hence the thermal stability plays crucial role to identify the applicability of the title crystal for distinct high-end laser devices. The melting point of GG crystal has been determined by means of differential thermal analysis (DTA) using the thermal analyzer (Linseis STA-PT 1600). The DTA thermogram of GG crystal has been recorded within 30–600 °C by employing the temperature rate of 10 °C/min. The recorded DTA thermogram of GG crystal is shown in Fig. 5. It shows the occurrence of sharp endothermic peak centered at 266.8 °C which resembles to the melting point of GG crystal. The absence of any peak below 100 °C confirms that the GG crystal does not possess water molecules. The single sharp peak confirms the good crystalline nature of GG crystal. It is also noticeable that the melting point of grown GG crystal is significantly higher than L-threonine crystal (262 °C) [59].

## 4. Conclusion

The GG crystal of dimension 17 × 10 × 06 $mm^3$ has been successfully grown by slow solvent evaporation technique. The single crystal XRD analysis confirmed the hexagonal structure and non-centrosymmetric $P3_1$ space group of GG crystal. The good crystalline phase of GG crystal has been ascertained from observed sharp peaks in PXRD pattern. The constituent elements of GG crystal have been qualitatively determined by means of EDS technique. In UV–visible analysis the GG crystal is found to exhibit high transmittance of 79% with optical energy band gap of 5.28 eV. The PL studies revealed that the GG crystal exhibits prominent violet colored emission with peak maxima centered at 343 nm. The SHG efficiency of GG crystal is found to be 5.06 times higher than KDP crystal owing to asymmetric structure and dipolar nature of grown crystal. Dielectric studies revealed that the magnitude of dielectric constant and dielectric loss increases with rise in temperature but significantly decreases with increase in frequency. In DTA analysis the sharp and single endothermic peak established the presence of single phase and confirmed the melting point of GG crystal at 266.8 °C. The grown GG crystal with impressive optical, dielectric and thermal properties pronounce its utmost credibility for designing components for photonics, optoelectronics, frequency convertors and distinct NLO devices.

## Acknowledgements

Author Mohd Anis acknowledges UGC, New Delhi, India for awarding Maulana Azad National Fellowship [F1-17.1/2015-16/MANF-2015-17-MAH-68193]. Author G.G. Muley is thankful to DST-SERB, India for the sanctioning major project (SB/EMEB-328/2013).

## References

[1] Z.H. Sun, D. Xu, X.Q. Wang, G.H. Zhang, G. Yu, L.Y. Zhu, H.L. Fan, Mater. Res. Bull. 44 (2009) 925–930.
[2] Xiaojing Liu, Zeyan Wang, Guanghui Zhang, Guangwei Yu, Aidong Duan, Xinqiang Wang, Dong Xu, Curr. Appl. Phys. 9 (2009) 22–25.
[3] Mohd Shkir, Haider Abbas, Spectrochem. Acta A 118 (2014) 172–176.
[4] L. Wang, G. Zhang, X. Liu, X. Wang, L. Wang, L. Zhu, D. Xu, Cryst. Res. Technol. 48 (2013) 1087–1096.
[5] G. Albercht, R.B. Corey, J. Am. Chem. Soc. 61 (1939) 1087–1103.
[6] E. Fischer Ber, Deut. Chem. Ges. 38 (1905) 2914–2917.
[7] Yoichi Iitaka, Proc. Jpn. Acad. 30 (1954) 109–112.
[8] E. Ramachandran, K. Baskaran, S. Natarajan, Cryst. Res. Technol. 42 (2007) 73–77.
[9] Yoichi Iitaka, Acta Cryst. 11 (1958) 225–226.
[10] Yoichi Iitaka, Acta Cryst. 14 (1961) 1–10.
[11] Mohd Anis, M.S. Pandian, M.I. Baig, P. Ramasamy, G.G. Muley, Mater. Res. Innov. (2017), http://dx.doi.org/10.1080/14328917.2017.1329992.
[12] T. Balakrishnan, R.R. Babu, K. Ramamurthi, Spectrochem. Acta A 69 (2008) 1114–1118.
[13] G.R. Dillip, P. Raghavaiah, K. Mallikarjuna, C. Madhukar Reddy, G. Bhagavannarayana, V. Ramesh Kumar, B. Deva Prasad Raju, Spectrochem. Acta A 79 (2011) 1123–1127.
[14] M. Esthaku Peter, P. Ramasamy, Spectrochem. Acta A 75 (2010) 1417–1421.
[15] P.V. Dhanaraj, N.P. Rajesh, Mater. Chem. Phys. 115 (2009) 413–417.
[16] S. Anbu Chudar Azhagan, S. Ganesan, Optik 124 (2013) 6456–6460.
[17] Mohd Anis, S.S. Hussaini, M.D. Shirsat, R.N. Shaikh, G.G. Muley, Mater. Res. Express 3 (2016) 106204–106210.
[18] G. Bhagavannarayana, S. Parthiban, S. Meenakshisundaram, J. Appl. Crystallogr. 39 (2006) 784–790.
[19] V.G. Pahurkar, Mohd Anis, M.I. Baig, S.P. Ramteke, B. Babu, G.G. Muley, Optik 142 (2017) 421–425.
[20] K. Rajesh, A. Arun, A. Mani, P.P. Kumar, Phys. Scr. 3 (2016) 106203–106213.
[21] B. Helina, P. Selvarajan, A.S.J. Lucia Rose, Phys. Scr. 85 (2012) 55803–55808.
[22] M. Sauer, J. Hofkens, J. Enderlein, Handbook of Fluorescence Spectroscopy and Imaging, Wiley-VCH Verlag GmbH & Co. KGaA, Weinheim, 2011.
[23] Y.B. Rasal, Mohd Anis, M.D. Shirsat, S.S. Hussaini, Mater. Res. Innov. (2017), http://dx.doi.org/10.1080/14328917.2017.1327199.
[24] Senthilkumar Chandran, Rajesh Paulraj, P. Ramasamy, Mater. Res. Bull. 68 (2015) 210–215.
[25] Mohd Anis, G.G. Muley, V.G. Pahurkar, M.I. Baig, S.R. Dagdale, Mater. Res. Innov. (2016), http://dx.doi.org/10.1080/14328917.2016.1264848.
[26] M.S. Kajamuhideen, K. Senthuraman, K. Ramamurthi, P. Ramasamy, Opt. Laser Technol. 91 (2017) 159–165.
[27] R.N. Shaikh, Mohd Anis, M.D. Shirsat, S.S. Hussaini, Mater. Technol. Adv. Perform. Mater. 19 (2015) 187–191.
[28] T.H. Gfroerer, Photoluminescence in Analysis of Surfaces and Interfaces, Encyclopedia of Analytical Chemistry, John Wiley& Sons Ltd, Chichester, 2000, pp. 9209–9231.
[29] S.L. Kakani, Amit Kakani, Materials Science, New Age International, New Delhi, 2004, pp. 417–419.
[30] R.N. Shaikh, Mohd Anis, M.D. Shirsat, S.S. Hussaini, J. Optoelectron. Adv. Mater. 16 (2014) 1147–1152.
[31] M.J. Weber, Handbook of Optical Materials, CRC Press, New York, 2003.
[32] M.S. Pandian, N. Pattanaboonmee, P. Ramasamy, P. Manyum, J. Cryst. Growth 314 (2011) 207–212.
[33] M.I. Baig, Mohd Anis, G.G. Muley, Optik 131 (2016) 165–170.

[34] Mohd Anis, G.G. Muley, Phys. Scr. 91 (2016) 85801–85808.
[35] R.O. Priakumari, S.G.S. Sheba, M. Gunasekaran, Mater. Res. Innov. 20 (2016) 177–181.
[36] M.I. Baig, Mohd Anis, G.G. Muley, Opt. Mater. 72 (2017) 1–7.
[37] A. Zamara, K. Rajesh, A. Thirugnanam, P.P. Kumar, Optik 125 (2014) 6082–6086.
[38] K.M. Priyadarshini, A. Chandramohan, G.A. Babu, P. Ramasamy, Sol. Stat. Sci. 28 (2014) 95–102.
[39] Y.B. Rasal, Mohd Anis, M.D. Shirsat, S.S. Hussaini, Mater. Res. Innov. 21 (2017) 45–49.
[40] S.K. Kurtz, T.T. Perry, J. Appl. Phys. 39 (1968) 3698–3813.
[41] M. Delfino, Mol. Cryst. Liq. Cryst. 52 (1979) 271–284.
[42] M. Lawrence, J.P. Thomas, Spectrochem. Acta A 91 (2012) 30–34.
[43] Artur Wojciechowski, Naser Alzayed, Iwan Kityk, Janusz Berdowski, Zbigniew Tylczyński, Opt. Appl. XL (2010) 1007–1012.
[44] G.R. Dillip, G. Bhagavannarayana, P. Raghavaiah, B.D.P. Raju, Mater. Chem. Phys. 134 (2012) 371–376.
[45] B.N. Moolya, A. Jayarama, M.R. Sureshkumar, S.M. Dharmaprakash, J. Cryst. Growth 280 (2005) 581–586.
[46] M.L. Caroline, G. Mani, S. Kumaresan, M. Kumar, S. Tamilselvan, G.J.S. Sundar, Optoelectron. Adv. Mater. Rapid Comm. 9 (2015) 1239–1244.
[47] Neeti Goel, Nidhi Sinha, Binay Kumar, Opt. Mater. 35 (2013) 479–486.
[48] M.I. Baig, Mohd Anis, G.G. Muley, Optik 131 (2017) 165–170.
[49] S.M. Azhar, Mohd Anis, S.S. Hussaini, S. Kalainathan, M.D. Shirsat, G. Rabbani, Mater. Sci. Pol. 34 (2016) 800–805.
[50] Preeti Singh, Mohd Hasmuddin, M.M. Abdullah, Mohd. Shkir, M.A. Wahab, Mater. Res. Bull. 48 (2013) 3926–3933.
[51] S.P. Ramteke, Mohd Anis, M.I. Baig, V.G. Pahurkar, G.G. Muley, Optik 137 (2017) 31–36.
[52] B.M. Boaz, M. Palanichamy, Babu Varghese, C.J. Raj, S.J. Das, Mater. Res. Bull. 43 (2008) 3587–3595.
[53] Mohd Anis, S.S. Hussaini, M.D. Shirsat, Optik 127 (2016) 9734–9737.
[54] R.C. Miller, Appl. Phys. Lett. 5 (1964) 17–19.
[55] Min-hua Jiang, Qi Fang, Adv. Mater. 11 (1999) 1147–1151.
[56] Mohd Anis, G.G. Muley, M.I. Baig, S.S. Hussaini, M.D. Shirsat, Mater. Res. Innov. (2016), http://dx.doi.org/10.1080/14328917.2016.1265250.
[57] Mohd Anis, M.I. Baig, G.G. Muley, S.S. Hussaini, M.D. Shirsat, Optik 127 (2016) 12043–12047.
[58] R.N. Shaikh, Mohd Anis, G. Rabbani, M.D. Shirsat, S.S. Hussaini, Optoelectron. Adv. Mater. Rapid Comm. 10 (2016) 526–531.
[59] G.R. Kumar, S.G. Raj, Adv. Mater. Sci. Eng. (2009), http://dx.doi.org/10.1155/2009/704294.